Article

Multi-Level Data Analyses in the Gajevo Landslide Research, Croatia

Laszlo Podolszki *, Luka Miklin [ID], Ivan Kosović and Vlatko Gulam

Croatian Geological Survey, Sachsova 2, 10000 Zagreb, Croatia
* Correspondence: lpodolszki@hgi-cgs.hr; Tel.: +385-916144705

Abstract: The Gajevo landslide is located in a hilly area of northern Croatia, where numerous landslides endanger and damage houses, roads, water systems, and power lines. Nevertheless, available landslide data are relatively scarce. Therefore, the Gajevo landslide location was chosen for detailed research and the development of a typical landslide model for this area. During initial research, the geographical and geological settings were reviewed and historical orthophotos were analysed. Due to the complexity and vulnerability of the area, the location required detailed investigations and the integration of multi-level data: remote (based on high-resolution LiDAR data) and field landslide mapping were performed and a map of the landslide area was developed. Precipitation data were reviewed, while shallow boreholes with material sampling and geophysical measurements provided information on material characteristics and 3D (depth) insight. As a result, knowledge was gained about material resistivity and composition along with the depth of sliding surfaces, and an engineering geological map of the Gajevo landslide area with the landslide and directly endangered areas marked was developed to be used by the local community in landslide risk assessment. As it is reasonable to expect that an extreme rainfall event will occur in combination with snowmelt in the coming years, resulting in the reactivation of Gajevo landslide, further research and continuous landslide monitoring are recommended.

Keywords: multi-level data; landslide research; remote sensing; geophysical data; engineering geology; precipitation trends

1. Introduction

Landslides can be described as the movement of a mass of rock, earth, or debris down a slope [1,2]. Slope movements are subdivided into six categories (falls, topples, slides, lateral spreads, flows, and composites) given their wide difference in mechanical behaviour [3–8]. The analysis and determination of the relationship between high precipitation events and the appearance of instabilities together with the review and comparison of the evolution of landslides locally and regionally aided by a multidisciplinary approach is also the object of important research worldwide [9–11]. The relationship between high precipitation events and the appearance of landslides has been discussed by various authors [12–14]. The higher the intensity of rain, the higher the pore pressure in the soil, resulting in a decrease in shear resistance [15]. As slides in the soil, i.e., clay/silt rotational, planar, or compound slides or gravel/sand debris slides [16], are most common in northern Croatia precipitation trends have a considerable impact on landslide activation [14,15].

The research area (Figure 1) of Gajevo landslide is located in northern Croatia (Figure 1a) in Zagreb County (ZgC), south of Zagreb city (Zg), within a hilly area that is prone to landslides (Figure 1b) [17]. There are many landslides in the wider area and as a result of these movements, houses, roads, water systems, and power lines have been endangered and damaged [18]. As the available landslide data for the hilly area of Vukomeričke Gorice are scarce, but landslides are relatively common [19], the Gajevo landslide location was chosen for detailed research and the development of a typical landslide model for

this area. The developed model could be used in mitigation processes, as it provides a better understanding of landslide mechanisms in the wider area in the same or similar conditions. The current trend in landslide investigations is a multi-level approach with data integration [20–24], and examples with results obtained via the synergy between the usage of remote sensing data, geophysical data, and geographical information systems are encouraging [15,25–29].
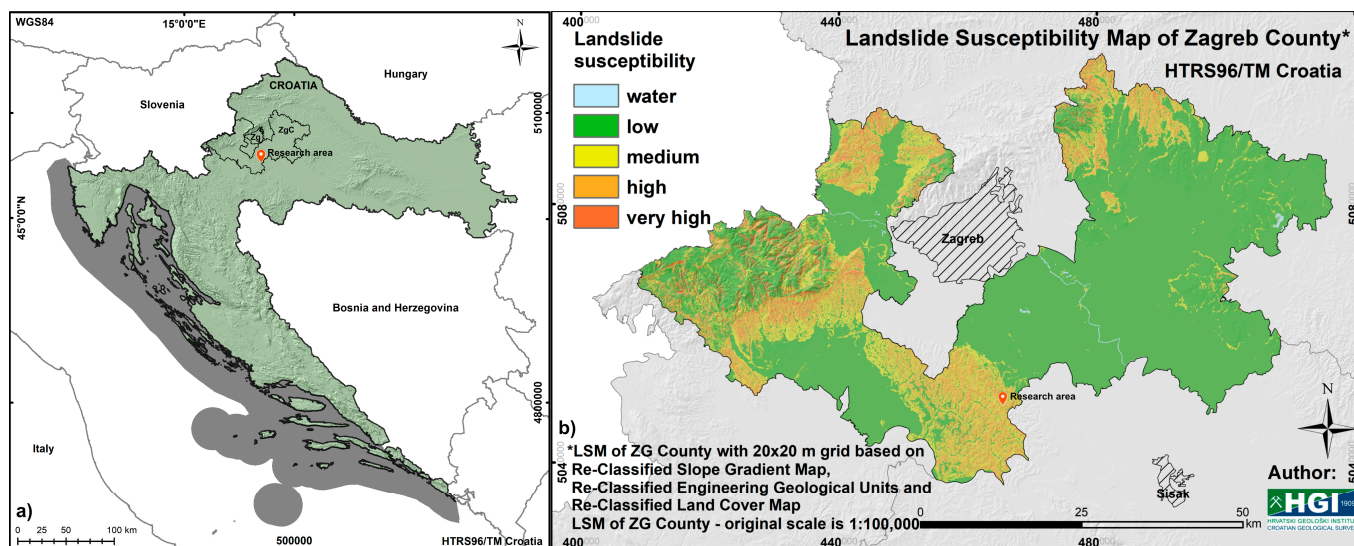

Figure 1. Research area location: (**a**) in northern Croatia south of Zagreb city (Zg) in Zagreb County (ZgC); (**b**) Landslide susceptibility map of Zagreb County, where the research area is found within the zones with medium to high landslide susceptibility [17].

Initial research into the Gajevo landslide location was performed based on pre-existing data: geographical and geological settings were reviewed, and historical orthophotos and available precipitation data were analysed [30]. In addition, remote (based on high resolution LiDAR data) and field landslide mapping were performed and an initial engineering geological map of the landslide area with cross-sections was developed [31]. In this initial research, an analysis of precipitation and temperature data helped to determine the time and cause of landslide activation, and a preliminary geological model with engineering–geological units and the definition of directly endangered area for households was presented [31].

However, due to the complexity and vulnerability of the area, the location required more detailed investigation. Thus, the goal of the research presented here was to prove the initial hypotheses with more detailed and concrete evidence from shallow boreholes with material sampling (3D data, in depth, vertical component), to upgrade and update the engineering geological map/cross-sections/model of the Gajevo landslide (in accordance with the available detailed remote sensing data) with geophysical measurement results, reach conclusions from a laboratory analysis of the borehole samples and to establish the monitoring of rainfall (collected data) with a pluviometer installed in the landslide area.

2. Materials and Methods

2.1. Engineering Geological Mapping—Integrating Multi-Level Data

The detailed geological setting for the wider area is described in [31]; however, it is still important to mention that the Gajevo landslide is located within informal Vrbova fm. [18], in which three major units can most often be differentiated: (i) sands with silts; (ii) clays with silts; and (iii) sands with gravels. Often, these units interchange and a "clean" boundary between them is hard to determine in the field due to the different ratios of "sandy" and "clayish" materials, i.e., their mixtures. Nevertheless, the material properties dictate water permeability, i.e., the engineering geological conditions: "It is often the case

that the sand/clay contact is a water-permeable/water-impermeable zone where, due to high pore-water pressures, the slide surface occurs and this is also the case with the Gajevo landslide [31]". This thesis was confirmed in the field by mapping (the landslide occurred on a sand/clay contact that was distinguishable on field) and historical orthophotos, and a precipitation analysis revealed that a high amount of precipitation in combination with snowmelt in February 2014 was the landslide's main triggering factor [31].

For the Gajevo landslide, an initial engineering geological map was developed based on available high-resolution remote sensing data and field mapping (described in detail in [31]); however, due to the complexity of the location, more detailed investigations were required, involving additional mapping with shallow boreholes (up to 5 m in depth, borehole locations are shown in Figure 2) and material sampling. In addition, for better 3D insight (in depth, vertical component) geophysical measurements were applied and three electrical resistivity tomography (ERT) cross-sections were developed. The ERT1-3 locations are shown in Figure 2. These investigations aimed to increase our knowledge of material properties, collect information about the depth/vertical component, and integrate the acquired multi-level data for the development/upgrade of the Gajevo landslide engineering geological map/landslide model.
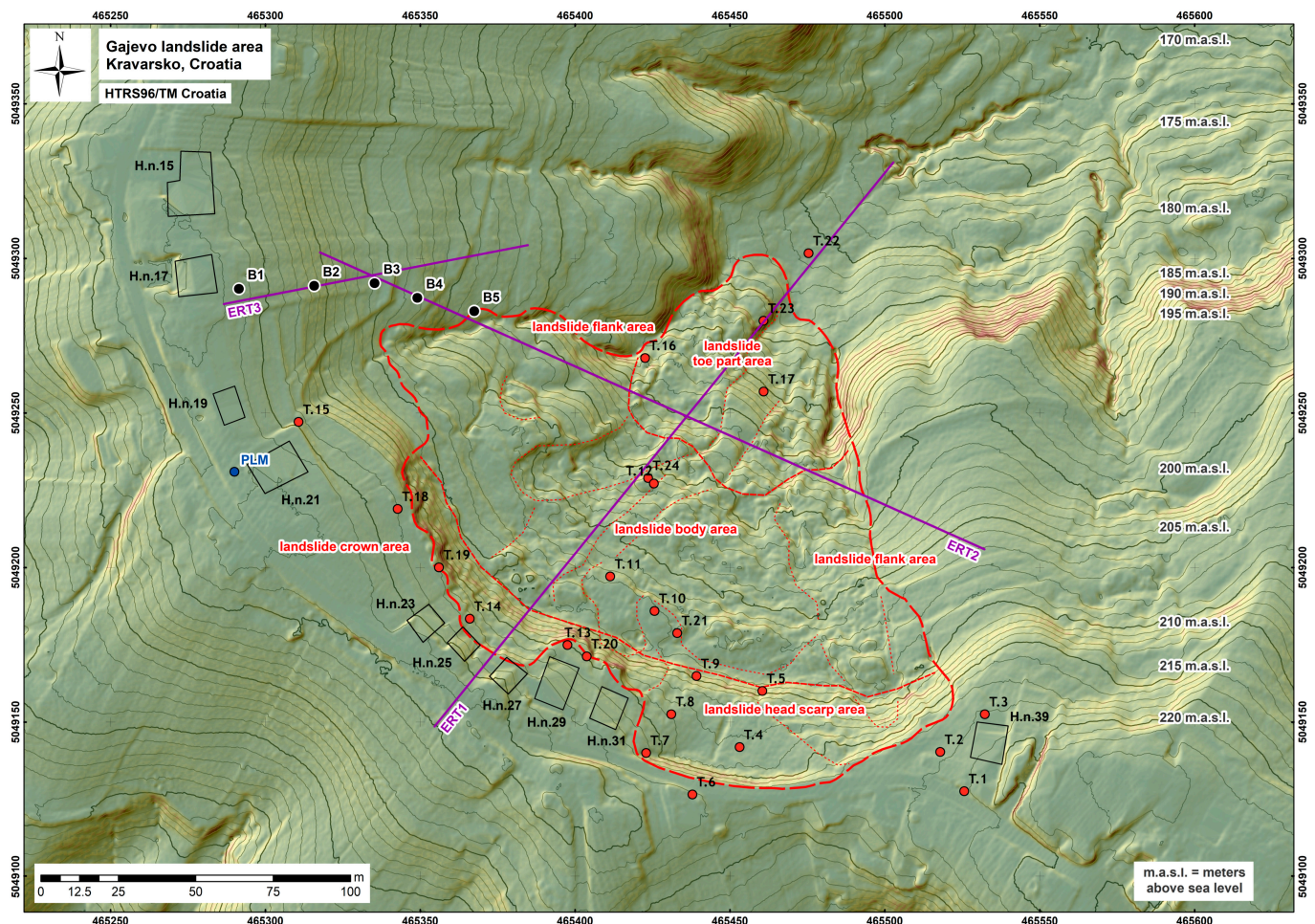

Figure 2. Gajevo landslide area overview with marked landslide features on high-resolution terrain slope model (0.5 × 0.5 m) with visible terrain morphology and locations of the ERT1–3 cross-sections (cross-section markings are placed at cross-sections starting points), boreholes (B1–5), installed pluviometer (PLM), field points (T1–24) used in mapping and houses "above" the landslide (house numbers 15–31 and 39). Multiple smaller landslides/deformations/cracks within the area of the initial landslide are also marked by thin red dashed lines.

2.2. Geophysical Measurements—ERT in Landslide Research

In comparison to other geophysical methods, ERT has a wide range of resistivity values, has a high correlation between electrical resistivity and lithology, provides the required depth of exploration, and evaluates the subsurface in 2D, 2.5D, and 3D [32,33]. This makes ERT applicable in geotechnical and geological research [25,26,34,35]. The ERT method, in addition to other near-surface geophysical methods, is widely used for the assessment and forecasting of landslide processes [36–39].

ERT measures the subsurface resistivity distribution via measurements made at the surface [26,40,41]. Soil resistivity varies as moisture content changes and/or when materials differ [15,42,43]. In theory, sands and clays can be differentiated, and the difference in resistivity between a dry soil and a saturated soil is significant [26,44,45]. In some cases, ERT measurements can provide data on the geometry of the landslide, and the depth of the sliding can be assessed [15,26,33,44].

With these assumptions in mind, three ERT cross-sections were developed in the Gajevo landslide area: one parallel to the movement (ERT1), one perpendicular to the movement (ERT2), and one in close vicinity of the landslide (ERT3), Figure 2. The aim was to obtain relevant data with field measurements (Figure 3), including the geometry of the landslide and the depth of the sliding from ERT1 and ERT2 and the "undisturbed/real" soil parameters from ERT3 (Figure 3a,b) and the shallow boreholes placed outside the landslide area (Figure 3c,d).

The ERT measurements were carried out using a multi-electrode resistivity system. Field measurements were performed using a POLARES 2.0 electrical imaging system (P.A.S.I. srl), which uses a sinusoidal alternate current with an adjustable frequency. This system was connected to 48 stainless steel electrodes, which were laid out in a straight line with a constant spacing of 5 m via a multi-core cable for ERT1 and ERT2. For ERT3 64 stainless steel electrodes with a constant spacing of 1.5 m were used. Surveys were conducted using the Wenner–Schlumberger array at a frequency of 1.79 Hz and a maximum phase of 20° between the voltage signal and the current signal. During the field measurements, the frequency was lowered until the number of incorrect measurements was below 10%. The RES2DINV resistivity inversion software [46] was used to automatically invert the apparent resistivity data from the field into resistivity subsurface models to provide information about the depth/vertical component. The absolute RMS error, which provides a measure of convergence between the measured and calculated data and thus indicates the reliability of the final result, was 3.3% for ERT1, 3.0% for ERT2, and 3.4% for ERT3. The resistivity datasets collected in the field were converted to ERT cross-sections, which were used for the interpretation of subsurface conditions: for ERT1 and ERT2, the length of a cross-section was ~235 m with an exploration depth of ~40 m, while for ERT3, the length of a cross-section was ~94.5 m with an exploration depth of ~20 m.

2.3. Laboratory Analysis

Although material characteristics were determined in the field, 18 samples from five boreholes were collected with the intention of choosing representative samples for further laboratory analysis (Figure 3e). Six samples were chosen for particle size distribution analysis (granulometry) to determine the ratios of sand/silt/clay and six samples were chosen for X-ray diffraction on powder (XRDP) to determine the presence and type of clay minerals: the results of three XRDP sample analysis are presented in this paper (see Section 3.3).

Figure 3. Overview of some field activities in Gajevo landslide area: (**a**) location of ERT3 cross-section outside landslide area; (**b**) measurement in progress on ERT3; (**c**) shallow borehole development; (**d**) borehole core determination; (**e**) borehole core sampling; (**f**) installed on-site pluviometer.

2.4. Precipitation Data

In the already-performed initial research, an analysis of precipitation data from the relevant surrounding meteorological stations (Pisarovina, Zagreb, Sisak, and Kravarsko) helped to determine the time and cause of landslide activation [31]. However, as the water content in the landslide body greatly affects its stability, on-site precipitation data monitoring was established at Gajevo landslide with a fixed pluviometer for further monitoring/research (Figure 3f). In addition, the available precipitation data from Kravarsko Meteorological Station were updated and reviewed once more, and new insights were reached (see Sections 3.4 and 4.4).

3. Results

3.1. Updated Engineering Geological Map

The engineering geological map of the Gajevo landslide area is presented in Figure 4. It is based on available existing geological data [47–52], high-resolution remote sensing data [31], data collected in the field, and laboratory analysis results.
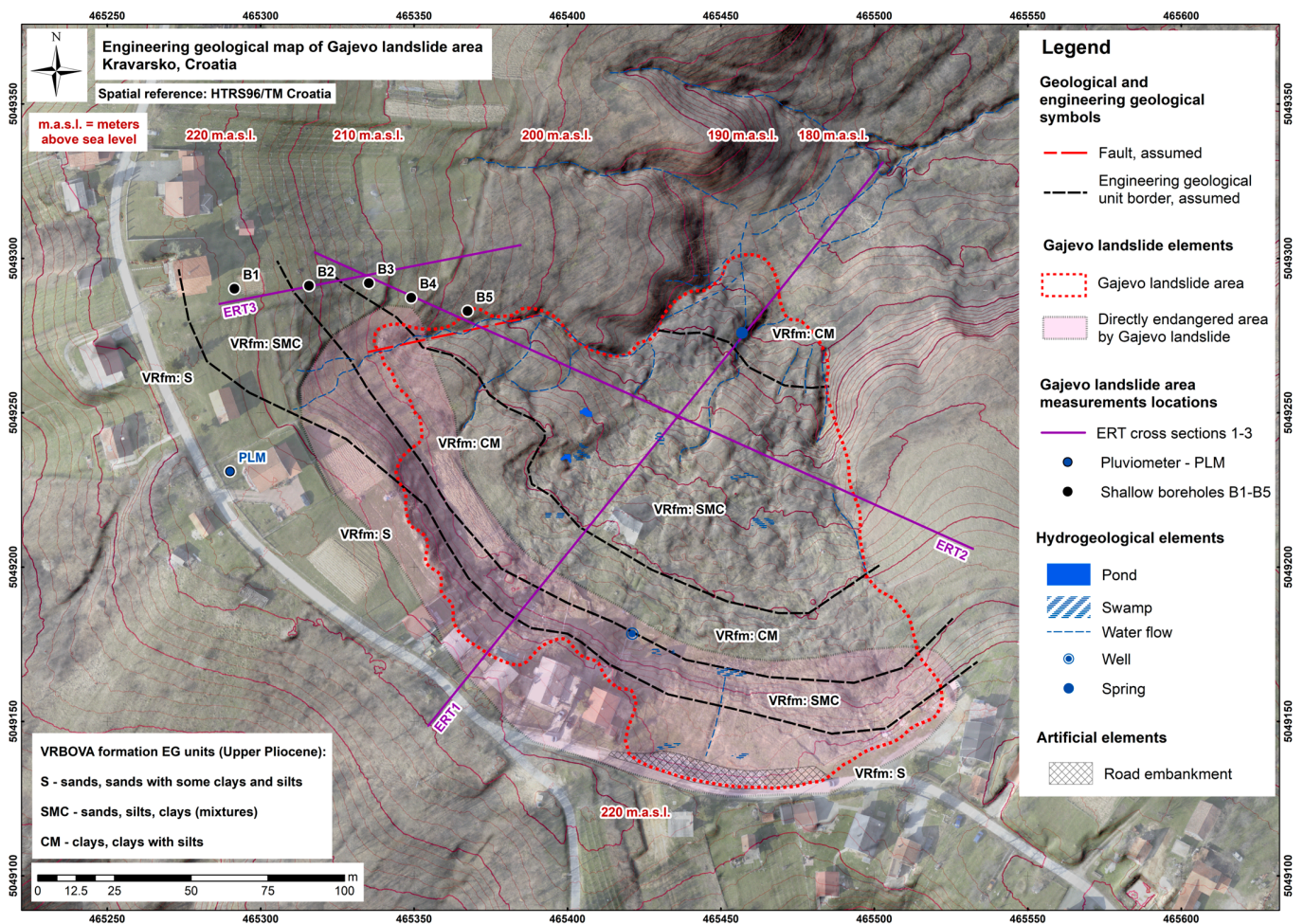

Figure 4. Updated engineering geological map of Gajevo landslide area with high-resolution orthophotos (10 × 10 cm pixel size) and a high-resolution digital elevation model (0.5 × 0.5 m cell size DEM) used as a base map. From the map is visible that five houses "above" the landslide in the vicinity of ERT1 are directly endangered. The ERT1–3 cross-section markings are placed at the cross-sections starting points.

In the Gajevo landslide area, the Upper Pliocene sediments of the informal Vrbova formation are present and can be divided into three engineering geological (EG) units based in on-site material characteristics (Figure 4): (i) sands, sands with some clays and silts (S); (ii) sands, slits, clays (mixtures, SMC); and (iii) clays, clays with silts (CM). The presented differentiation of units the in informal Vrbova fm. is somewhat different from the standard (see Section 2.1) due to the actual conditions present in the field. To vindicate the "used" EG units for the Gajevo area, samples were taken from shallow boreholes and a laboratory analysis was conducted (see Section 3.3) and the resulting map (Figure 4) is somewhat different/modified/updated than the map presented in [31].

From an engineering point of the view, the stability of the area is important, and for the Gajevo landslide area, this stability mostly depends on the water content in the "soil". All superficial water "appearances" were marked/mapped, and from these data, the most important was the position of the well (208 m above sea level) on the contact of "mixtures" and "clayish" materials right below the head scarp area. Within the well, the water level was found on the terrain surface, indicating the groundwater level, i.e., the landslide body downslope is probably still (mostly) saturated.

The landslide area is ~19,500 m^2 with a height difference of ~35 m. The head scarp height varies between ~5 and 10 m and extends along the road for ~225 m. The landslide is located on the northern side of the slope, where the main movement direction is northeast [31]. The landslide is considered as a composite [4], with multiple smaller landslides/deformations/cracks within the area of the initial landslide (Figure 2).

Considering all of the available data (and newly recorded minor deformations and cracks developed during the period/process of field mapping from 2019 to 2022), future movements are expected in the Gajevo landslide area and a directly endangered area (critical zone) can be defined as the area in the vicinity of the existing head scarp, where the road and five houses are in the critical zone (house numbers 23–31). This endangered area is ~11,000 m^2 and encompasses both areas that are already in movement (landslide area) and the area without (major) signs of instabilities (landslide crown area).

3.2. Developed ERT Cross-Sections with Borehole Data

For the Gajevo landslide area, the 3D (depth/vertical component) data are scarce thus, the ERT cross-sections developed here provide valuable information. From ERT1 (Figure 5) and ERT2 (Figure 6), it can be seen that the material in movement (colluvial material) is relatively close to the surface: with lower resistivity values up to ~40–50 Ωm and generally speaking, as the depth increases the resistivity is higher. On the "western" side of ERT2 (around boreholes B4 and B5), there is a zone near the surface with lower resistivity values, which could indicate a weakened zone/fault area. This zone can be identified on the terrain by geomorphological/topographical indicators (V-shaped valley with stream, changes in contour lines, and also indicative is the landslide border position, Figure 4) but was not visible in the material (changes) from the shallow boreholes: the material in boreholes B4 and B5 was mostly a heterogeneous mixture of sands, silts, and clays.

ERT3 (Figure 7) was placed outside the landslide area with the intention of obtaining "undisturbed/real" soil parameters; however, the cross-section was complex to interpret as its resistivity values changed "irregularly". Still, it could be explained in the following way: (i) sandy layers had a greater resistivity value (>70 Ωm) with "purer" sandy layers having higher resistivity values (>100 Ωm); (ii) relatively low resistivity values were observed at the middle part of the cross-section at a depth of ~10 m (<20 Ωm, Figure 7, which could be an indication of the influence of a weakened zone/fault area and/or the presence of "clayish" materials and/or high water content; and (iii) material interchanges (sands vs. silts vs. clays) were irregular and common for a relatively small area/depth.
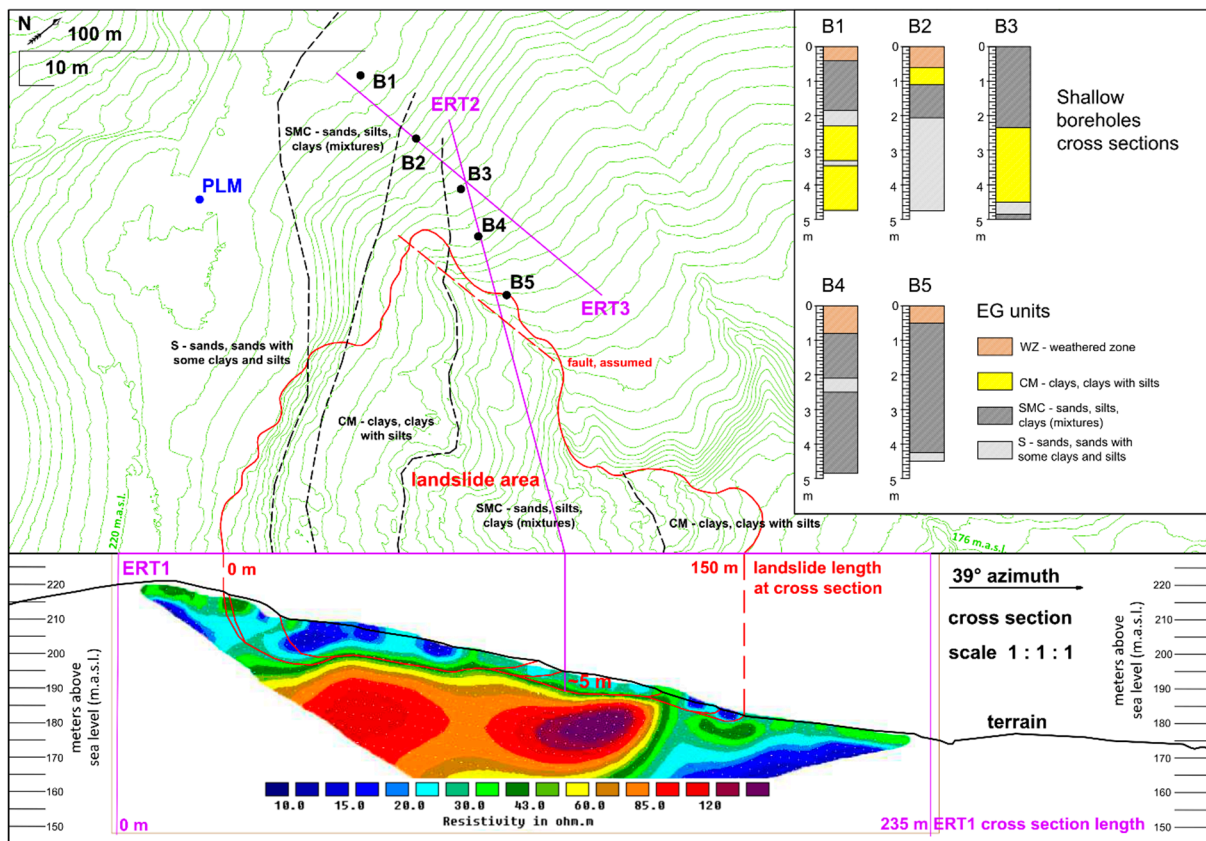
Figure 5. Sliding surfaces depth interpretation at ERT1 and borehole data (B1–B5).
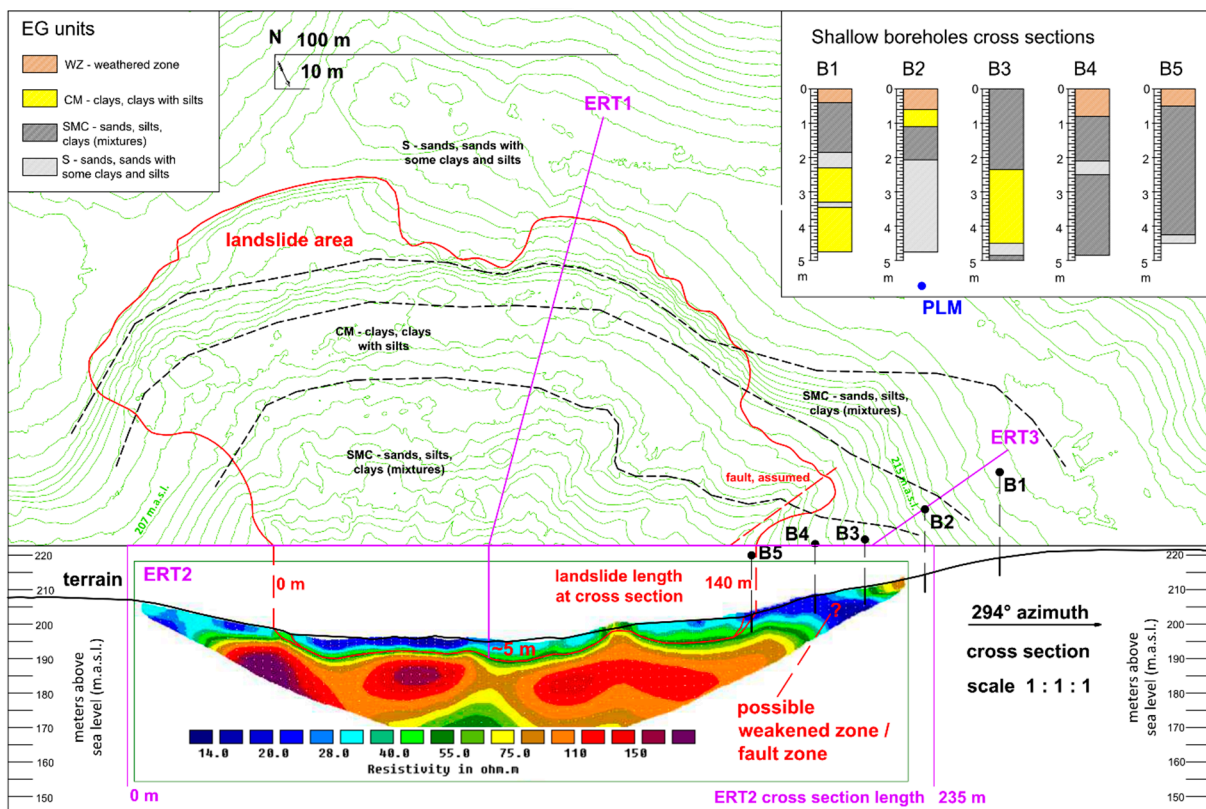

Figure 6. Sliding surfaces depth interpretation at ERT2 with a possible weakened zone in the vicinity of B4 and B5.
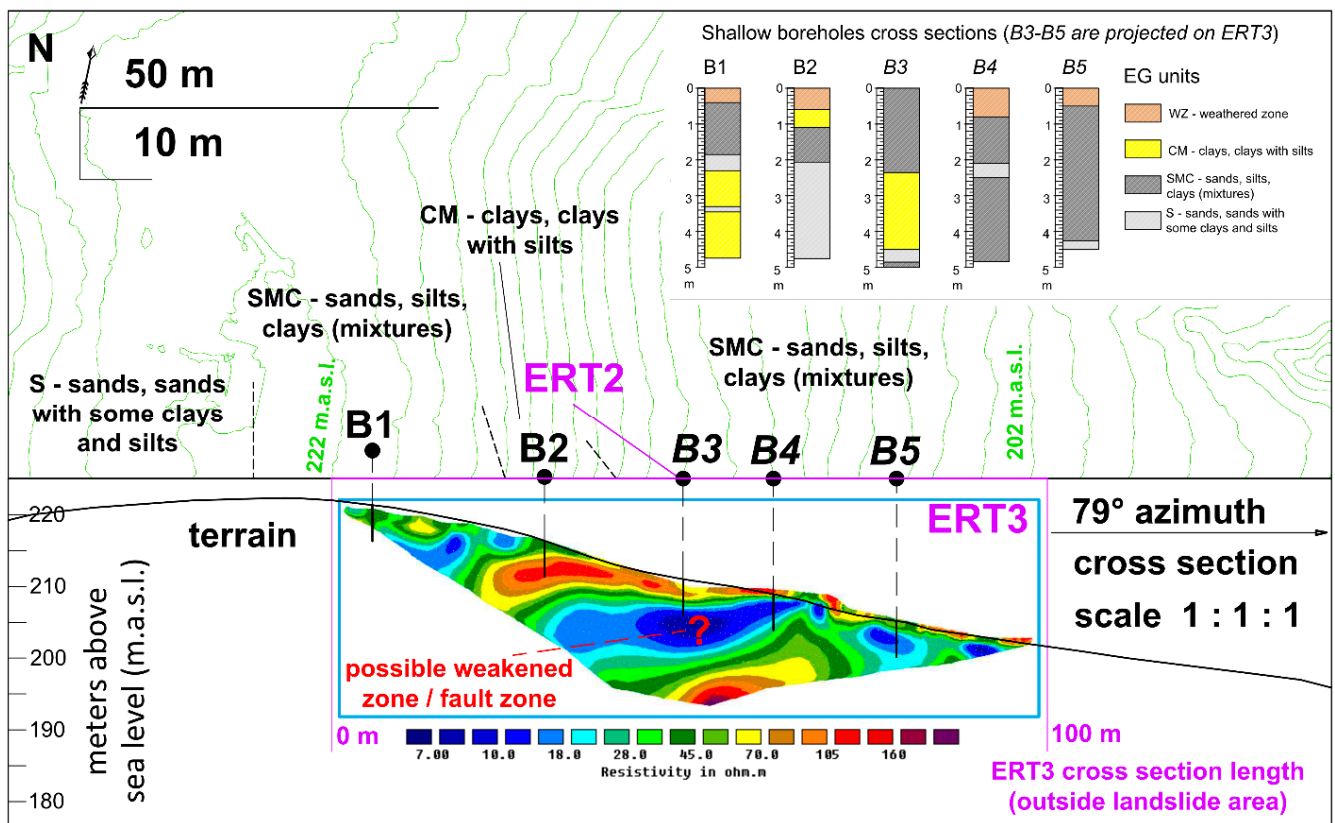
Figure 7. Material properties at ERT3 and B1–B5: outside the landslide area.

From the interpreted ERT1 and ERT2 information about material resistivity and sliding surfaces depth can be gained: ~5 m at the middle part of the landslide and ~10 m at the upper part of the landslide (Figures 5 and 6). From the ERT2 and ERT3 data, a possible weakened zone/fault area could be interpreted where the material resistivity values are low (Figures 6 and 7).

In boreholes B1–B5 (Figures 5–7), there was a shallow weathered zone (up to ~0.8 m of depth, described as "top soil with roots"), after which material mixtures (sands, slits, clays) followed (up to ~2 m of depth for B1–B3 and greater for B4 and B5). Sandy layers were present at a depth of ~2 m in B1, B2, and B4 and below a depth of ~4 m in B3 and B5. Clayish layers were more pronounced in B1 and B3 at a depth below ~2.3 m, and there was a relatively thin clayish layer in B2 at a depth of 0.6–1.1 m. The possible weakened zone/fault area is in the vicinity of the B4 and B5 (Figures 6 and 7), which could be the reason why "only" material mixtures were recorded in the B4 and B5 core samples (with some thin sandy layers), while in B1, B2, and B3 more "rhythmic" material interchanges were present (Figures 5–7).

3.3. Laboratory Analysis Results

Samples for laboratory analysis were taken from the shallow boreholes to clarify and verify the material characteristics determined in the field, i.e., the EG units used.

The particle size distribution (granulometry) of six samples was analysed to determine the ratios of sand vs. silt vs. clay. The laboratory analysis for these six samples was carried out in accordance with field material determination/classification, and the actual ratios (laboratory test results [53]) are shown in Table 1. Samples B1–S1 and B3–S4 can be considered as "typical" sand-silt-clay mixtures where more than 20% of one material type but less than 50% of the "dominant" material type was present in the sample [54]. Sample B1–S2 was "typical" silt-clay, almost "pure". Samples B2–S3, B3–S5, and B5–S6 were variants of sandy materials with an "emphasized coarse grain component" (~60%

or more), and with ~30% of silt and some clay (up to ~10%). For each EG unit used, a representative sample was analysed (Figure 4): (i) sands, sands with some clays and silts (S), represented by samples B2–S3, B3–S5, and B5–S6; (ii) sands, slits, clays (mixtures SMC), represented by samples B1–S1 and B3–S4; and (iii) clays, clays with silts (CM), represented by sample B1–S2, as shown in Table 1. It should be pointed out that sands, silts, and clays were present in all six analysed samples; however, the sand ratios varied from 363%, silts ratios varied from 32–59% and clays ratios varied from 5–38%. The particle size distribution analysis was performed according to the ASTM-D422-63 norm [55].

Table 1. Particle size distribution with classification for the six analysed samples.

Sample	Depth (m)	Gravel, G (%)	Sand, S (%)	Silt, M (%)	Clay, C (%)	Classification
B1–S1	1.65–1.75	0.0	37.9	34.1	28.0	SMC
B1–S2	2.65–2.75	0.0	3.1	58.7	38.3	CM
B2–S3	2.85–2.95	0.0	62.5	32.8	4.7	S with M
B3–S4	1.80–1.90	0.0	23.9	47.1	29.0	SMC
B3–S5	4.70–4.80	0.0	59.3	33.6	7.1	S with M
B5–S6	4.30–4.40	13.3	44.4	32.1	10.2	S with M

An additional analysis was performed on samples with larger "silty" and "clayish" components (samples B1–S1, B1–S2, and B3–S4). The analysis was performed according to the ASTM-D-2216-19 norm [56] to determine water content (W_0) and the ASTM-D4318-17 norm [57] to determine the liquid limit (W_L), plastic limit (W_P), plasticity index (I_P) and consistency index (I_C), as shown in Table 2. According to the classification presented in Table 2, samples B1–S1 and B3–S4 are medium plastic clays (CI), while sample B1–S2 is a highly plastic clay (CH). The presented material classifications differ slightly between Tables 1 and 2 as different laboratory tests were used; however, the results/material properties indicate the same—the presence of clay: in the B1–S1 (SMC) sample there was 28% clay and in the B3–S4 (SMC) sample there was 29% clay, and those clays were medium plastic, while in the B1-S2 (CM) sample there was 38% clay and that clay is highly plastic. The presence of high shrink-swell capacity clay was also confirmed by the X-ray diffraction on powder (XRDP) analysis results [58].

Table 2. Water content, Atterberg limits, and plasticity and consistency indexes with classification for three analysed samples.

Sample	Depth (m)	W_0 (%)	W_L (%)	W_P (%)	I_P (%)	I_C (-)	Classification
B1–S1	1.65–1.75	24.8	46	23	23	0.92	Cl
B1–S2	2.65–2.75	24.2	53	27	26	1.10	CH
B3–S4	1.80–1.90	22.4	47	23	24	1.02	Cl

X-ray diffraction on powder (XRDP) analysis was performed for three samples [58]. The samples were taken from borehole B1 at a depth of 4.70 m, B2 at a depth of 0.75 m, and B3 at a depth of 2.95 m. The results showed the presence of quartz, calcite, muscovite, chlorite, and clay minerals (vermiculite, montmorillonite, kaolinite, and illite) in all three samples [58]. These findings are in accordance with those of previously conducted research in the *Viviparus* beds/Vrbova fm., where the mineral composition of the <2 μm fraction ("clay size minerals") included chlorite, illite/muscovite, and kaolinite [59]. However, vermiculite and montmorillonite clay minerals were additionally identified in the analysed samples from the Gajevo landslide area [58]. Montmorillonite is a characteristic component of "swelling/expansive soil", i.e., it is a clay with a high shrink–swell capacity.

3.4. Analysis of Precipitation Data from Kravarsko Meteorological Station

Initial precipitation data are described in [31], where February 2014 was determined as the date of Gajevo landslide activation. The landslide was activated due to a combination of temperature increases (from -2 °C on the 1 February to 11 °C on the 16 February), which caused snowmelt, accompanied by heavy rains (240 mm of precipitation in February, of which 85 mm fell on the 12 February 2014).

As precipitation was the main landslide trigger [31] in this case (in combination with snowmelt), available precipitation data from Kravarsko Meteorological Station for 2000–2021 (the last 22 years, Table 3) were further reviewed in the context of ongoing climate changes [12,60]. From the precipitation data (Table 3), the following interpretations could be made: (i) yearly precipitation values showed a general increasing trend (Figure 8), especially if periods 2000–2012 and 2013–2021, with average precipitation values of 765 mm and 1087 mm are compared); (ii) there were extremes in the period of 2000–2021, with the "dry" year corresponding to 2011 and the "wet" year represented by 2014 (when the landslide occurred); and (iii) precipitation minimum and maximum values (months) varied widely through the year(s). As these precipitation amounts (values) changed, the general trend (for this part of continental Croatia) with "drier" (from March to August) and "wetter" (from September to February) parts of the year is hard to follow (Figure 8); however, this trend was still visible for 2000, 2001, 2003, 2007, 2009, and 2010 and for the period of 2012–2021 (except 2018). For 2002, 2004, 2005, 2006, and 2011, there was a higher amount of precipitation in the period from March to August, similar to that observed in 2008 and 2018 but with less pronounced differences.

Table 3. Precipitation data from Kravarsko Meteorological Station for the period of 2000–2021.

Year	Precipitation (mm/year) [1]	Precipitation Minimum (Monthly Values)	Precipitation Maximum (Monthly Values)
2000	638	9 mm in August	119 mm in December
2001	973	22 mm in October	216 mm in September
2002	952	21 mm in January	149 mm in April
2003	578	3 mm in March	116 mm in October
2004	903	42 mm in January	190 mm in April
2005	954	28 mm in January	169 mm in August
2006	750	5 mm in October	171 mm in August
2007	797	4 mm in April	156 mm in October
2008	613	13 mm in May	99 mm in March
2009	614	14 mm in September	89 mm in June
2010	973	41 mm in December	167 mm in September
2011	478 [2]	1 mm in November	93 mm in June
2012	728	5 mm in March	125 mm in December
2013	966	23 mm in July	163 mm in January
2014	1601 [3]	43 mm in March	265 mm in September
2015	1047	4 mm in December	216 mm in October
2016	1107	2 mm in December	169 mm in February
2017	1001	37 mm in July	237 mm in September
2018	980	18 mm in August	177 mm in February
2019	1234	31 mm in February	215 mm in May
2020	917	7 mm in January	189 mm in October
2021	930	2 mm in June	138 mm in October

[1] Average (yearly) precipitation for Kravarsko Meteorological Station for 2000–2021 is 897 mm. [2] 2011 was an extremely "dry" year. [3] 2014 was an extremely "wet" year.
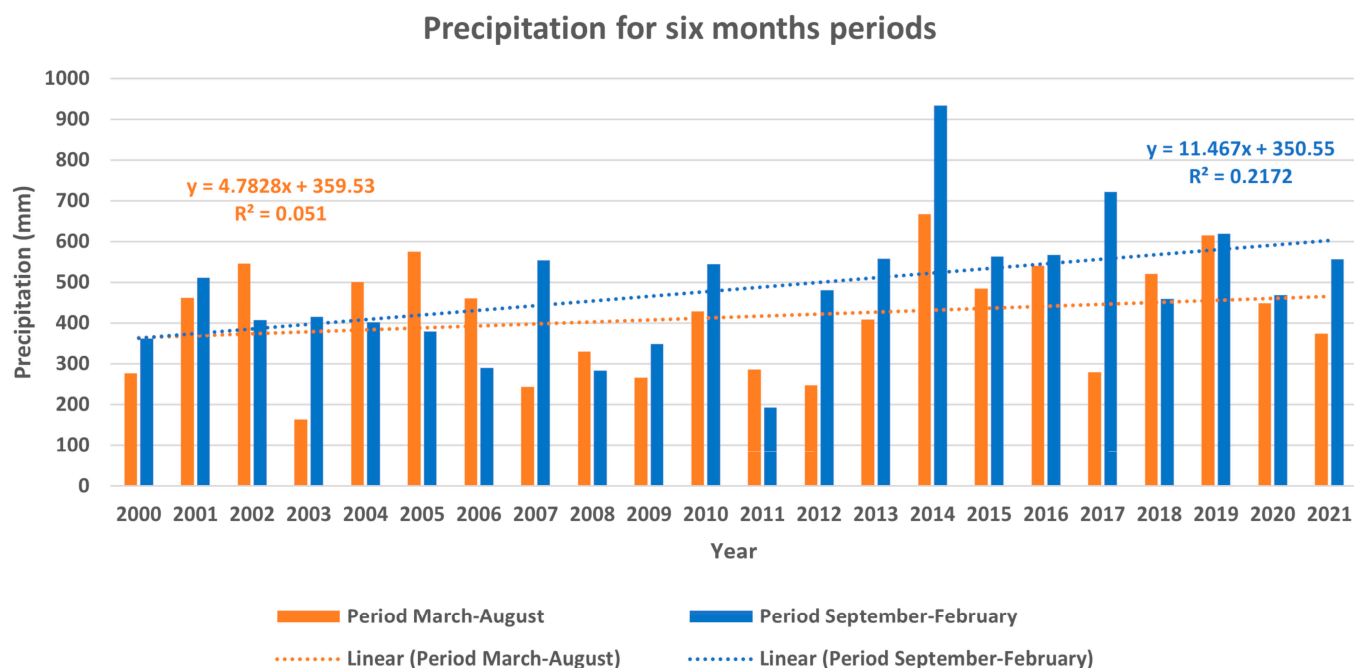
Figure 8. Precipitation for six-month periods from Kravarsko Meteorological Station for the period of 2000–2021.

The need for continuous monitoring is apparent as: (i) precipitation minimums and maximums varied in their amounts and time of occurrence; (ii) yearly precipitation values increased (general increasing trend, that became more pronounced from 2013 onwards, which we consider as evidence of ongoing climate changes); and (iii) more extreme events are expected ("dry" and "wet" years), and with them the reactivation of the Gajevo landslide.

4. Discussion

Landslides can be devastating and fatal [61]. To avoid these scenarios and to minimize the negative effects of landslides, multidisciplinary research into landslides is carried out: (i) determine the spatiotemporal evolution of landslides [62]; (ii) measure landslide morphometry and areal changes by remote sensing [63]; (iii) develop ground models [64]; and (iv) develop remedial measures [65].

A recent landslide that resulted in the endangerment of safety and extensive property damage in Croatia was the Hrvatska Kostajnica landslide in 2018. In that case, a multi-level approach to landslide research provided valuable insights [15] and guidelines on how to proceed when previous landslide data were practically non-existent.

As available landslide data for the wider research area (the Vukomeričke Gorice hilly area [18]) and landslide locality (Gajevo [30]) are scarce, multi-level data analyses were carried out for the Gajevo landslide research area as follows: (i) with the usage of field mapping and remote sensing data, a preliminary map of Gajevo landslide area was developed [30] and updated (Figure 4); (ii) with ERT measurements, knowledge about material resistivity and sliding surface depth was gained (Figures 5–7); (iii) material characteristics determined in the field were confirmed by laboratory analysis [53,58]; and (iv) an analysis of precipitation trends showed that more extreme events are expected (Tables 3 and 4, Figure 8). All of these findings are valuable novelty for the Gajevo landslide area. It is important to note that as the reactivation of the Gajevo landslide due to extreme events (rainfall with snowmelt) is possible in the future, the landslide map provided here (Figure 4) can be used in the development of mitigation plans for the endangered area/critical zone.

Table 4. Precipitation values of ≥40 mm per heavy rainfall event (h.r.e.) at Kravarsko Meteorological Station for the period of January 2000–September 2022.

Year	February	March	April	May	June	July	August	September	October	November	December	No. of h.r.e. [1]
2001										41		1
2006										41		1
2010								42				1
2014	**85**			43		49	47	40	**64**			6
2015				67			69			52		3
2016					**82**							1
2017								40, **60**	48			3
2018		40	48		**73**							3
2019					46, 53			**97**		53		4
2020							57, 58	45	58			4
2021									41		40	2
2022			46	49					no data	no data	no data	2

[1] Years (2000, 2002–2005, 2007–2009, and 2011–2013) and months (January) without heavy rainfall events are not presented in the table (there were only three h.r.e. in the period of 2000–2012, these values are marked in italics). For the period of January 2000–September 2022, there were 31 h.r.e. with five events having ≥60 mm of rainfall (bolded values) and three extreme events with ≥80 mm of rainfall (2014, 2016, and 2019, red bolded values).

4.1. Comments on the Developed Engineering Geological Map of the Gajevo Landslide Area

Informal Vrbova fm. sediments are present in the Gajevo landslide area. Within this area three EG units could be differentiated on site (Figure 4): (i) "sandy sediments" (S); (ii) "clayish sediments" (CM); and (iii) their mixtures (SMC) [46,47]. These units interchange and vary both laterally and vertically, thus, it is hard to map them. The used EG units were somewhat different than the standard units used for the informal Vrbova fm. ("sandy", "clayish", and "gravely" [45]); however, they were site-appropriate and backed up by laboratory analysis results (see Section 3.3) [46,47].

The presented map (Figure 4) is simplified in comparison with the initial map presented in [24] with respect to EG units, and in addition, the area directly endangered by the Gajevo landslide was modified (enlarged), as additional field mapping was carried out and new data were acquired (ERT and borehole data with laboratory analysis results).

The developed engineering geological map of the Gajevo landslide area with the landslide and directly endangered areas marked is already in a form that the local community can use in landslide risk assessment [66]: the road and five houses are directly endangered, and three more houses are near the landslide area (Figure 4).

4.2. Gajevo Landslide Area 3D Data Review

New ERT and borehole data provided "vertical" (3D, depth) information about the Gajevo landslide area. Information about material resistivity and sliding surface depth was gained from ERT1 and ERT2 [18,22,26]: ~5 m at the middle part of the landslide and ~10 m at the upper part of the landslide (Figures 5 and 6). In ERT2 and ERT3, a possible weakened zone/fault area could be interpreted where material resistivity values are low (Figures 6 and 7) [25,26]. In general, the material resistivity values were low for the Gajevo landslide area, and it was hard to distinguish different layers (EG units) in the ERT cross-sections; however, the landslide features (sliding surface depth) could be interpreted, which represent an information of great value in landslide research.

The shallow boreholes were placed outside the landslide area on purpose (Figure 4) to obtain as much information as possible about the "undisturbed" sediment distribution and to try to identify the mapped EG units for the area in the borehole core(s), Figures 5–7. This was accomplished as the distinct EG units for the area were identified in the shallow borehole core samples. As mentioned earlier, even though the EG units interchange and vary both laterally and vertically, the previously mapped data (2D) are in accordance

with the acquired borehole data (3D) and as such provide a valuable verification for the developed map.

4.3. Gajevo Landslide Area Material Properties Findings

The Gajevo landslide area materials can be described as sands, silts, and clays (see Section 3.3). The site-specific location characteristics depend on material ratios: sand vs. silt vs. clay. These ratios are hard to determine in the field, samples and laboratory analysis are needed. As "sandy" materials are more permeable than "clayish" materials upon contact between these layers sliding often occurs in Vrbova fm. [11], just as it occurred at the Gajevo landslide location.

It is worth mentioning that in some cases, the presence of highly plastic expansive clays can "influence" the behaviour of the "rest" of the silty-clayish component, where the whole sample "acts unfavourable" from the aspect of stability [47,67]. In addition, the material's water content is important with respect to stability and can be correlated with electrical conductivity/resistivity. Higher water content indicates a low resistivity value and high conductive zone, while lower water content indicates high resistivity and low conductivity value [68]. The resistivity values of "sandy" materials are generally higher than those of "clayish" materials. However, they are influenced by water content: "sandy" materials with water can have resistivities in the range of 100–150 Ωm [69] and "clayish" materials with water can have resistivities lower than 100 Ωm [70].

As mentioned previously, the effect of water content and the degree of saturation [71], soil structure [72] and pore fluid [73] can affect material resistivity values. However, for the Gajevo landslide area, the following general interpretations can be made: (i) with increasing depth, material resistivity values also increase; (ii) materials with resistivity values > 100 Ωm can be interpreted as predominantly "sandy" materials; and (iii) near-surface materials within landslide area with resistivity values < 40 Ωm can be interpreted as colluvial material.

Due to the material properties present in the Gajevo landslide area (sediment characteristics presented in Tables 1 and 2), the determination of EG units is not possible solely based on ERT even in undisturbed materials. For these types of complex sediments/mixtures, detailed field mapping and laboratory analysis are needed [46,51]. If available, high-resolution remote sensing data (high-resolution DEMs and orthophotos) can also help, as on it, distinct geomorphological and landslide features can be identified, which in some cases can also indicate a change in material properties.

4.4. Importance of Heavy Rainfall Events

As heavy rainfall events (h.r.e.) are the most common trigger of landslides in northern Croatia [11,74], daily h.r.e. were singled out for the period of January 2000–September 2022 from the available (daily) data of Kravarsko Meteorological Station (Table 4). A threshold value for h.r.e. precipitation of ≥40 mm cumulative rainfall per day was set. The data showed that for the period of 2000–2012, only three h.r.e. were recorded (with relatively low values for daily precipitation of 41, 41, and 42 mm of rain, Table 4). For the period of 2013–2022, there were 28 h.r.e. with five daily precipitation values ≥ 60 mm (60, 64, 67, 69 and 73 mm of rain, Table 4) and three extreme events with >80 mm of precipitation in one day (82, 85, and 97 mm of rain, Table 4). Generally, yearly precipitation values increased (period of 2013–2022, Table 3) and there were more months with a higher amount of (cumulative) rainfall and more "critical" heavy rainfall events [35,53]. As these events are spread throughout the year without a visible pattern, continuous precipitation monitoring is needed.

The h.r.e. from February 2014 with 85 mm of rain (in combination with snowmelt) was the main triggering factor of the Gajevo landslide. It is indicative that the other two extremes occurred when snow cover was not present, in the summer of 2016 (June, 85 mm of rain) and in the autumn of 2019 (September, 97 mm of rain), and "only" caused minor movements in the Gajevo landslide body: the measured deformations on houses on Gajevo

Street were within centimetres range [23]. From the available data, it can be concluded that: (i) the frequency of h.r.e. and the amount of precipitation per event has increased, and extreme events are continuing to happen; (ii) the intensity and timing of these events cannotbe predicted; (iii) from the aspect of slope stability, extreme events are important; and (iv) it is reasonable to expect an extreme event to occur in combination with snowmelt in the coming years, i.e., the reactivation of the Gajevo landslide. The authors consider the presented data interpretation as evidence of ongoing climate changes and from the aspect of slope stability these trends are negative.

4.5. Landslide Mitigation Plan Guidelines

As a first step, "water control" must be established in the critical zone to minimize the entrance of water into the landslide body, with the development and establishment of adequate road and houses drainage systems as follows: (i) gutters should be checked, cleaned, or installed; (ii) shallow channel systems with material replacements should be developed around houses; and (iii) deeper drainage pipes with geo-textiles should be developed in the landslide body, for example, the "fishbone" construction type could be applied. As a result, the water can be gathered and steered away to the existing stream downslope in a controlled way. However, further detailed research with landslide monitoring is recommended for the development of an efficient mitigation plan that can be put in place. The installation of an on-site pluviometer can be considered as step taken towards continuous landslide monitoring.

5. Conclusions

The presented Gajevo landslide can be considered as a typical simplified landslide model in the Vrbova fm. The landslide occurred on sand/clay contact due to an increase in pore water pressures. It was triggered by a heavy rainfall event (85 mm of rain), which coincided with a temperature change from -2 °C to 11 °C and snowmelt in February 2014. It is a relatively large composite landslide with an area of ~19,500 m^2 and a height difference of ~35 m. The head scarp height varies between 5 and 10 m, and it extends along the road for ~225 m. The landslide is located on the northern side of the slope, where its main movement is in the northeast direction, and it is still directly endangering the road at the top of the slope and five houses.

The sliding surface depth was interpreted from the ERT cross-sections of the landslide area as ~5 m at the middle part of the landslide and ~10 m at the upper part of the landslide. Overall, the material resistivity values from the ERT's were low and it was hard to distinguish the different layers (engineering geological units) as the materials (sand vs. silt vs. clay) interchange and vary both laterally and vertically, therefore field mapping was performed and samples were collected for laboratory analysis from shallow boreholes outside the landslide area. Based on the available data, three engineering geological units were differentiated on site: (i) "sandy sediments"; (ii) "clayish sediments"; and (iii) their mixtures, as presented on the developed engineering geological map of the Gajevo landslide area. The developed map, with the landslide and directly endangered areas marked, is already in a form that the local community can use for landslide risk assessment and urban planning. The establishment of water drainage systems along the road, on and around houses with gutters and shallow channels is recommended as an urgent mitigation measure in the critical zone.

As the authors interpret it, the precipitation trends for the Kravarsko area are being influenced by the ongoing climate changes: (i) Yearly precipitation values showed a general increasing trend, especially when the periods of 2000–2012 and 2013–2020 with average precipitation values of 765 mm and 1107 mm are compared); (ii) there were extremes in the period of 2000–2020, with a "dry" year in 2011 (with 478 mm of precipitation) and a "wet" year in 2014, when landslide occurred (with 1601 mm of precipitation); and (iii) precipitation minimum and maximum values (months) varied widely through the year(s). In addition, for the period of 2000–2012, only three heavy rainfall events were

recorded, while for the period of 2013–2020, there were 28 heavy rainfall events, with 5 rainfalls having ≥60 mm of precipitation and three extreme events with >80 mm of precipitation. As these trends are negative from the perspective of slope stability (precipitation values are increasing), it is reasonable to expect an extreme rainfall event to occur in combination with snowmelt in the coming years, resulting in the reactivation of the Gajevo landslide, which could endanger the properties and the safety of residents.

The need for further research is imperative along with continuous landslide monitoring in order to develop successful forecasting and early warning systems.

References

1. Cruden, D.M. A simple definition of a landslide. *Bull. Int. Assoc. Eng. Geol.* **1991**, *43*, 27–29. [CrossRef]
2. The International Geotechnical Societies' UNESCO Working Party on World Landslide Inventory (WP/WLI). A suggested method for reporting a landslide. *Bull. Int. Assoc. Eng. Geol.* **1990**, *41*, 5–12. [CrossRef]
3. Chacón, J.; Irigaray, C.; Fernández, T.; El Hamdouni, R. Engineering Geology Maps: Landslides and Geographical Information Systems. *Bull. Eng. Geol. Environ.* **2006**, *65*, 341–411. [CrossRef]
4. Cornforth, D.H. *Landslides in Practice: Investigation, Analysis, and Remedial/Preventative Options in Soils*; John Wiley & Sons, Inc.: Hoboken, NJ, USA, 2005; pp. 1–596, ISBN 978-0-471-67816-8.
5. Cruden, D.M.; Varnes, D.J. Landslide types and processes. In *Landslides—Investigation and Mitigation*; Turner, A.K., Schuster, R.L., Eds.; Transportation Research Board: Washington, DC, USA, 1996; Special Report 247; pp. 36–75. Available online: http://onlinepubs.trb.org/Onlinepubs/sr247/sr247-003.pdf (accessed on 25 October 2022).
6. Highland, L.M.; Bobrowsky, P. *The Landslide Handbook—A Guide to Understanding Landslides*; US Geological Survey: Denver, CO, USA, 2008; pp. 1–147. [CrossRef]
7. Varnes, D.J. Slope movement types and processes. In *Landslides: Analysis and control*; Schuster, R.L., Krizek, R.J., Eds.; Transportation Research Board. National Academy of Sciences: Washington, DC, USA, 1978; Special Report 176; pp. 11–33. Available online: https://www.engr.hk/T05/176-002.pdf (accessed on 25 October 2022).
8. Varnes, D.J. *Landslide Hazard Zonation: A Review of Principles and Practice*; International Association of Engineering Geology: Paris, France, 1984; pp. 1–63.
9. Carrión-Mero, P.; Montalván-Burbano, N.; Morante-Carballo, F.; Quesada-Román, A.; Apolo-Masache, B. Worldwide Research Trends in Landslide Science. *Int. J. Environ. Res. Public Health* **2021**, *18*, 9445. [CrossRef]
10. de Ojeda, P.S.; Sanz, E.; Galindo, R. Historical reconstruction and evolution of the large landslide of Inza (Navarra, Spain). *Nat. Hazards* **2021**, *109*, 2095–2126. [CrossRef]
11. Esposito, G.; Carabella, C.; Paglia, G.; Miccadei, E. Relationships between Morphostructural/Geological Framework and Landslide Types: Historical Landslides in the Hilly Piedmont Area of Abruzzo Region (Central Italy). *Land* **2021**, *10*, 287. [CrossRef]
12. Araújo, J.R.; Ramos, A.M.; Soares, P.M.M.; Melo, R.; Oliveira, S.C.; Trigo, R.M. Impact of extreme rainfall events on landslide activity in Portugal under climate change scenarios. *Landslides* **2022**, *19*, 2279–2293. [CrossRef]
13. Calista, M.; Miccadei, E.; Piacentini, T.; Sciarra, N. Morphostructural, Meteorological and Seismic Factors Controlling Landslides in Weak Rocks: The Case Studies of Castelnuovo and Ponzano (North East Abruzzo, Central Italy). *Geosciences* **2019**, *9*, 122. [CrossRef]
14. Mihalić Arbanas, S.; Sečanj, M.; Bernat Gazibara, S.; Krkač, M.; Begić, H.; Džindo, A.; Zekan, S.; Arbanas, Ž. Landslides in the Dinarides and Pannonian Basin—From the largest historical and recent landslides in Croatia to catastrophic landslides caused by Cyclone Tamara (2014) in Bosnia and Herzegovina. *Landslides* **2017**, *14*, 1861–1876. [CrossRef]

15. Podolszki, L.; Kosović, I.; Novosel, T.; Kurečić, T. Multi-Level Sensing Technologies in Landslide Research—Hrvatska Kostajnica Case Study, Croatia. *Sensors* **2022**, *22*, 177. [CrossRef]

16. Hungr, O.; Leroueil, S.; Picarelli, L. The Varnes classification of landslide types, an update. *Landslides* **2014**, *11*, 167–194. [CrossRef]

17. Pollak, D.; Bostjančić, I.; Gulam, V. *CGS SafEarth Project Report: Landslide Susceptibility Map in Scale of 1:100,000—Zagreb County (Project ID: HR-BA-ME59, WP Implementation Deliverable: T1.3.2a, LSM in Small Scale (HGI), Annex 3 LSM in Small Scale for Zagreb County)*; Internal Data Base of Interreg—IPA CBC Croatia—Bosnia and Herzegovina—Montenegro, Croatian Geological Survey: Zagreb, Croatia, 2018; pp. 1–2, 1 map.

18. Podolszki, L.; Kurečić, T.; Bateson, L.; Svennevig, K. Remote Landslide Mapping, Field Validation and Model Development—An Example from Kravarsko, Croatia. *Geol. Croat.* **2022**, *75/1*, 67–82. [CrossRef]

19. Zagrebačka županija. Proglašena Elementarna Nepogoda Za Općinu Kravarsko [Zagreb County. Declared Natural Disaster for Kravarsko Municipality—In Croatian] (19.02.2014). Available online: https://www.zagrebacka-zupanija.hr/vijesti/1763/proglasena-elementarna-nepogoda-za-opcinu-kravarsko (accessed on 29 September 2022).

20. Blahůt, J.; Jaboyedoff, M.; Thiebes, B. "Novel Approaches in Landslide Monitoring and Data Analysis" Special Issue: Trends and Challenges. *Appl. Sci.* **2021**, *11*, 10453. [CrossRef]

21. Fall, M.; Azzam, R.; Noubactep, C.A. Multi-Method Approach to Study the Stability of Natural Slopes and Landslide Susceptibility Mapping. *Eng. Geol.* **2006**, *82*, 241–263. [CrossRef]

22. Guzzetti, F.; Mondini, A.C.; Cardinali, M.; Fiorucci, F.; Santangelo, M.; Kang-Tsung, C. Landslide inventory maps: New tools for an old problem. *Earth Science Reviews* **2012**, *112*, 42–66. [CrossRef]

23. Janeras, M.; Jara, J.A.; Royán, M.J.; Vilaplana, J.M.; Aguasca, A.; Fàbregas, X.; Gili, J.A.; Buxó, P. Multi-Technique Approach to Rockfall Monitoring in the Montserrat Massif (Catalonia, NE Spain). *Eng. Geol.* **2017**, *219*, 4–20. [CrossRef]

24. Soto, J.; Galve, J.P.; Palenzuela, J.A.; Azañón, J.M.; Tamay, J.; Irigaray, C. A multi-method approach for the characterization of landslides in an intramontane basin in the Andes (Loja, Ecuador). *Landslides* **2017**, *14*, 1929–1947. [CrossRef]

25. Grabar, K.; Miklin, Ž.; Strelec, S. Geotechnical investigations of the fortress "Minčeta", Dubrovnik, Croatia. *Inženjerstvo okoliša* **2016**, *3/2*, 63–72. Available online: https://hrcak.srce.hr/172502 (accessed on 25 October 2022).

26. Hussain, Y.; Schlögel, R.; Innocenti, A.; Hamza, O.; Iannucci, R.; Martino, S.; Havenith, H.-B. Review on the Geophysical and UAV-Based Methods Applied to Landslides. *Remote Sens.* **2022**, *14*, 4564. [CrossRef]

27. Jaboyedoff, M.; Del Gaudio, V.; Derron, M.-H.; Grandjean, G.; Jongmans, D. Characterizing and Monitoring Landslide Processes Using Remote Sensing and Geophysics. *Eng. Geol.* **2019**, *259*, 105167. [CrossRef]

28. Jaboyedoff, M.; Oppikofer, T.; Abellán, A.; Derron, M.H.; Loye, A.; Metzger, R.; Pedrazzini, A. Use of LIDAR in landslide investigations: A review. *Nat Hazards* **2012**, *61*, 5–28. [CrossRef]

29. Khan, M.Y.; Shafique, M.; Turab, S.A.; Ahmad, N. Characterization of an Unstable Slope Using Geophysical, UAV, and Geological Techniques: Karakoram Himalaya, Northern Pakistan. *Front. Earth Sci.* **2021**, *9*, 1–11. [CrossRef]

30. Miklin, L. Primjena metoda daljinskih istraživanja na klizištu Gajevo, Kravarsko [Application of Remote Sensing Methods on the Gajevo Landslide (Kravarsko)—In Croatian]. Master's Thesis, University of Zagreb, Zagreb, Croatia, 2021.

31. Miklin, L.; Podolszki, L.; Gulam, V.; Markotić, I. The impact of Climate Changes on Slope Stability and Landslide Conditioning Factors: An Example from Kravarsko, Croatia. *Remote Sens.* **2022**, *14*, 1794. [CrossRef]

32. Hung, Y.C.; Chou, H.S.; Lin, C.P. Appraisal of the Spatial Resolution of 2D Electrical Resistivity Tomography for Geotechnical Investigation. *Appl. Sci.* **2020**, *10*, 4394. [CrossRef]

33. Whiteley, J.S.; Watlet, A.; Uhlemann, S.; Wilkinson, P.; Boyd, J.P.; Jordan, C.; Kendall, J.M.; Chambers, J.E. Rapid characterisation of landslide heterogeneity using unsupervised classification of electrical resistivity and seismic refraction surveys. *Eng. Geol.* **2021**, *290*, 106189. [CrossRef]

34. Hasan, M.; Shang, Y.; Meng, H.; Shao, P.; Yi, X. Application of Electrical Resistivity Tomography (ERT) for Rock Mass Quality Evaluation. *Sci. Rep.* **2021**, *11*, 1–19. [CrossRef]

35. Lapenna, V.; Perrone, A. Time-Lapse Electrical Resistivity Tomography (TL-ERT) for Landslide Monitoring: Recent Advances and Future Directions. *Appl. Sci.* **2022**, *12*, 1425. [CrossRef]

36. Marescot, L.; Monnet, R.; Chapellier, D. Resistivity and induced polarization surveys for slope instability studies in the Swiss Alps. *Eng. Geol.* **2008**, *98*, 18–28. [CrossRef]

37. Huntley, D.; Bobrowsky, P.; Hendry, M.; Macciotta, R.; Elwood, D.; Sattler, K.; Best, M.; Chambers, J.; Meldrum, P. Application of multi-dimensional electrical resistivity tomography datasets to investigate a very slow-moving landslide near Ashcroft, British Columbia, Canada. *Landslides* **2019**, *16*, 1033–1042. [CrossRef]

38. Santoso, B.; Hasanah, M.U.; Setianto. Landslide investigation using self potential method and electrical resistivity tomography (Pasanggrahan, SouthSumedang, Indonesia). *IOP Conf. Ser.: Earth Environ. Sci.* **2019**, *311*, 1–9. [CrossRef]

39. Whiteley, J.S.; Chambers, J.E.; Uhlemann, S.; Boyd, J.; Cimpoiasu, M.O.; Holmes, J.L.; Inauen, C.M.; Watlet, A.; Hawley-Sibbett, L.R.; Sujitapan, C.; et al. Landslide monitoring using seismic refraction tomography—The importance of incorporating topographic variations. *Eng. Geol.* **2020**, *268*, 105525. [CrossRef]

40. Kumar, D. Efficacy of Electrical Resistivity Tomography Technique in Mapping Shallow Subsurface Anomaly. *J. Geol. Soc. India* **2012**, *80*, 304–307. [CrossRef]

41. Loke, M.H.; Rucker, D.F.; Chambers, J.E.; Wilkinson, P.B.; Kuras, O. Electrical Resistivity Surveys and Data Interpretation. In *Encyclopedia of Solid Earth Geophysics, Encyclopedia of Earth Sciences Series*; Gupta, H., Ed.; Springer: Cham, Switzerland, 2020. [CrossRef]

42. Bai, D.; Lu, G.; Zhu, Z.; Zhu, X.; Tao, C.; Fang, J. Using Electrical Resistivity Tomography to Monitor the Evolution of Landslides' Safety Factors under Rainfall: A Feasibility Study Based on Numerical Simulation. *Remote Sens.* **2022**, *14*, 3592. [CrossRef]

43. Ivanik, O.; Shabatura, O.; Khomenko, R.; Kravchenko, D.; Hadiatska, K. The application of the ERT method for the landslides investigation. *EAGE, Geoinformatics* **2021**, *2021*, 1–6. [CrossRef]

44. Hussain, Y.; Hamza, O.; Cárdenas-Soto, M.; Borges, W.R.; Dou, J.; Rebolledo, J.F.R.; Prado, R.L. Characterization of Sobradinho Landslide in Fluvial Valley Using MASW and ERT Methods. *REM Int. Eng. J.* **2020**, *73*, 487–497. [CrossRef]

45. Perrone, A.; Lapenna, V.; Piscitelli, S. Electrical Resistivity Tomography Technique for Landslide Investigation: A Review. *Earth-Science Rev.* **2014**, *135*, 65–82. [CrossRef]

46. Loke, M.H. *Tutorial: 2-D and 3-D Electrical Imaging Surveys*; Geotomo Software: Penang, Malaysia, 2020. Available online: https://www.geotomosoft.com/downloads.php (accessed on 30 August 2022).

47. Čubrilović, P.; Palavestrić, L.; Nikolić, T. *Inženjerskogeološka Karta Jugoslavije 1:500,000 [Engineering–Geological Map of Yugoslavia in Scale of 1:500,000—In Croatian]*; Geological Department of Serbia: Belgrade, Srbija, 1967.

48. Podolszki, L.; Pollak, D.; Gulam, V.; Miklin, Ž. Development of Landslide Susceptibility Map of Croatia. In *Engineering Geology for Society and Territory—Volume 2: Landslide Processes*; Lollino, G., Giordan, D., Crosta, G.B., Corominas, J., Azzam, R., Wasowski, J., Sciarra, N., Eds.; Springer: Berlin/Heidelberg, Germany, 2015; Volume 2, pp. 947–950. [CrossRef]

49. Bostjančić, I.; Filipović, M.; Gulam, V.; Pollak, D. Regional-Scale Landslide Susceptibility Mapping Using Limited LiDAR-Based Landslide Inventories for Sisak-Moslavina County, Croatia. *Sustainability* **2021**, *13*, 4543. [CrossRef]

50. Pikija, M. *Osnovna Geološka Karta SFRJ 1:100.000—List Sisak L33-93 [Basic Geological Map SFRY in Scale of 1:100,000—Sheet Sisak L33-93—In Croatian]*; Geological Department of Serbia: Belgrade, Serbia, 1987.

51. Pikija, M. *Osnovna Geološka Karta SFRJ 1:100.000—Tumač Za List Sisak L33-93 [Guide for Basic Geological Map SFRY in Scale of 1:100,000—Sheet Sisak L33-93—In Croatian]*; Geological Department of Serbia: Belgrade, Serbia, 1987.

52. Kurečić, T. Sedimentologija i Paleoekologija Pliocenskih Viviparus Slojeva Vukomeričkih Gorica a [Sedimentology and Paleoecology of Pliocene Viviparus Beds from the Area of Vukomeričke Gorice—In Croatian]. Ph.D. Thesis, University of Zagreb, Zagreb, Croatia, 2017.

53. Jović, A. *Laboratory Tests Report—Gajevo Landslide*; Geotehnički Studio d.o.o: Zagreb, Croatia, 2022; pp. 1–11.

54. *ASTM-D2487-06*; Standard Practice for Classification of Soils for Engineering Purposes (Unified Soil Classification System). American Society for Testing and Materials: West Conshohocken, PA, USA, 2010; pp. 1–12. [CrossRef]

55. *ASTM-D422-63*; Standard Test Method for Particle-Size Analysis of Soils. American Society for Testing and Materials: West Conshohocken, PA, USA, 2007; pp. 1–8. [CrossRef]

56. *ASTM-D2216-19*; Standard Test Methods for Laboratory Determination of Water (Moisture) Content of Soil and Rock by Mass. American Society for Testing and Materials: West Conshohocken, PA, USA, 2019; pp. 1–7. [CrossRef]

57. *ASTM-D4318-17*; Standard Test Methods for Liquid Limit, Plastic Limit, and Plasticity Index of Soils. American Society for Testing and Materials: West Conshohocken, PA, USA, 2018; pp. 1–20. [CrossRef]

58. Puškarić, A. *Laboratory Analysis Report—XRDP Qualitative Analysis of Samples from Gajevo Landslide*; Ruđer Bošković Institute: Zagreb, Croatia, 2022; pp. 1–4.

59. Kurečić, T.; Kovačić, M.; Grizelj, A. Mineral assemblage and provenance of the pliocene *Viviparus* beds from the area of Vukomeričke Gorice, Central Croatia. *Geol. Croat.* **2021**, *74/3*, 253–271. [CrossRef]

60. Leyva, S.; Cruz-Pérez, N.; Rodríguez-Martín, J.; Miklin, L.; Santamarta, J.C. Rockfall and Rainfall Correlation in the Anaga Nature Reserve in Tenerife (Canary Islands, Spain). *Rock Mech. Rock Eng.* **2022**, *55*, 2173–2181. [CrossRef]

61. Haque, U.; Blum, P.; da Silva, P.F.; Andersen, P.; Pilz, J.; Chalov, S.R.; Malet, J.P.; Jemec Auflič, M.; Andres, N.; Poyiadji, E.; et al. Fatal landslides in Europe. *Landslides* **2016**, *13*, 1545–1554. [CrossRef]

62. Bian, S.; Chen, G.; Zeng, R.; Meng, X.; Jin, J.; Lin, L.; Zhang, Y.; Shi, W. Post-failure evolution analysis of an irrigation-induced loess landslide using multiple remote sensing approaches integrated with time-lapse ERT imaging: Lessons from Heifangtai, China. *Landslides* **2022**, *19*, 1179–1197. [CrossRef]

63. Samodra, G.; Ramadhan, M.F.; Sartohadi, J.; Setiawan, M.A.; Christanto, N.; Sukmawijaya, A. Characterization of displacement and internal structure of landslides from multitemporal UAV and ERT imaging. *Landslides* **2020**, *17*, 2455–2468. [CrossRef]

64. Merritt, A.J.; Chambers, J.E.; Murphy, W.; Wilkinson, P.B.; West, L.J.; Gunn, D.A.; Meldrum, P.I.; Kirkham, M.; Dixon, N. 3D ground model development for an active landslide in Lias mudrocks using geophysical, remote sensing and geotechnical methods. *Landslides* **2014**, *11*, 537–550. [CrossRef]

65. Bednarik, M.; Putiška, R.; Dostál, I.; Tornyai, R.; Šilhán, K.; Holzer, F.; Weis, K.; Ružek, I. Multidisciplinary research of landslide at UNESCO site of Lower Hodruša mining water reservoir. *Landslides* **2018**, *15*, 1233–1251. [CrossRef]

66. Bell, F.G. *Geological Hazards: Their Assessments, Avoidance and Mitigation*; E&FN Spon Press: London, UK, 2003; pp. 1–648.

67. Qi, S.; Vanapalli, S.K. Influence of swelling behavior on the stability of an infinite unsaturated expansive soil slope. *Comput. Geotech.* **2016**, *76*, 154–169. [CrossRef]

68. Asriza, S.; Kristyanto, T.H.W.; Indra, T.L.; Syahputra, R.; Tempessy, A.S. Determination of the Landslide Slip Surface Using Electrical Resistivity Tomography (ERT) Technique. In *Advancing Culture of Living with Landslides. WLF 2017*; Mikos, M., Tiwari, B., Yin, Y., Sassa, K., Eds.; Springer: Cham, Switzerland, 2017. [CrossRef]
69. Pandey, L.M.S.; Shukla, S.K.; Habibi, D. Electrical resistivity of sandy soil. *Géotechnique Lett.* **2015**, *5*, 178–185. [CrossRef]
70. Telford, W.M.; Geldart, L.P.; Sheriff, R.E. *Applied Geophysics*; Cambridge University Press: New York, NY, USA, 1990; pp. 1–760. Available online: https://kobita1234.files.wordpress.com/2016/12/telford-geldart-sheriff-applied-geophysics.pdf (accessed on 25 October 2022).
71. Munoz-Castelblanco, J.A.; Pereira, J.M.; Delage, P.; Cui, Y.J. The influence of changes in water content on the electrical resistivity of a natural unsaturated loess. *Geotech. Test. J.* **2012**, *35/1*, 11–17. [CrossRef]
72. Fukue, M.; Minato, T.; Horibe, H.; Taya, N. The microstructures of clay given by resistivity measurements. *Eng. Geol.* **1999**, *54/1–2*, 43–53. [CrossRef]
73. Yoon, G.L.; Park, J.B. Sensitivity of leachate and fine contents on electrical resistivity variations of sandy soils. *J. Haz. Mater.* **2001**, *84/2–3*, 147–161. [CrossRef]
74. Mihalić Arbanas, S.; Krkač, M.; Bernat, S. Application of innovative technologies in landslide research in the area of the City of Zagreb (Croatia, Europe). Croatia. *Geol. Croat.* **2016**, *69/2*, 231–243. [CrossRef]